www.jatit.org

LOAD FLOW SOLUTION FOR ILL-CONDITIONED POWER SYSTEMS USING RUNGE- KUTTA AND IWAMOTO METHODS WITH FACTS DEVICES

S.Suresh Reddy **S.Sarat kumar** **Dr. S.V.J.Kumar**

ABSTRACT

This paper presents a load flow calculation method using Runge-Kutta and IWAMOTO methods for ill conditioned power systems with facts devices like SVC, TCSC, STATCOM, and UPFC. This paper shows that there is formal analogy between Newton's method and a set of autonomous ordinary differential equations. This analogy suggests that numerical integration method i.e., Runge-Kutta formulae can be used for solving the power flow problem. This paper uses the concept of optimal multiplier for solving the ill conditioned power systems with modification to the normal Newton-Raphson method in Iwamoto's method. To examine the effectiveness of proposed methods 13 bus ill conditioned system along with the steady state modeling of the devices (SVC,TCSC,STATCOM,UPFC) with their functional capabilities are observed.

Indexterms: *Ill-conditioned, IWAMOTO method,Newton-Raphson,method. SVC, TCSC, STATCOM, UPFC*

I. INTRODUCTION:

The power flow analysis is one of the most important problems in power system studies. The studies for the load flow calculations started with Ward and Hale method in 1956 [1] and currently the Newton Raphson method are being widely used [7], [8].

It is relevant to classify the power flow problems into following categories.

1. Well-conditioned case: The power flow solution exists and is reachable using a flat initial guess with a standard Newton-Raphson method. This case is the most common situation.
2. Ill-conditioned case: The solution of the power flow problem does exist but standard solution methods fail to get the solution starting from a flat initial guess. Typically this solution is due to the fact that the region of attraction of the power flow solution is narrow or far away from the initial guess. In this case, the failure of standard power flow solution methods is due to the instability of the numerical method, not of the power flow equations.

The difficulties which cause instability and divergence in load flow solution with Newton-Raphson method are,

1. Selection of reference slack bus
2. Existence of negative line resistance
3. High R/X ratio
4. Choosing initial values

IWAMOTO method has proved to be efficacious for solving ill conditioned cases.

To the best of our knowledge no attempt has been made in finding load flow solution with FACTS devices on ill-conditioned power systems which motivated us for this work.

II. Review of NR load flow

The power flow problem is formulated as a set of nonlinear equations, as follows:

$$g(x) = 0 \quad \text{----------(1)}$$

Where g and x are the variables, i.e. voltage amplitudes and voltage phases at load buses, reactive power and voltage phases at PV buses and active and reactive powers at the slack bus [13]. In classical power flow formulation, variables and equations are twice the number of network buses.

Since (1) are nonlinear and cannot be explicitly inverted, one has to use a numerical iterative technique for solving power flow problem. The i-th iteration of classical Newton-Raphson (NR) algorithm for (1) as follows:

$$\Delta x^i = -\left[g_x^i\right]^{-1} g^i \qquad \text{-(2)}$$

$$x^{(i+1)} = x^{(i)} + \Delta x^{(i)}$$

where $g_x = \nabla_x^T g$ is the Jacobian matrix of the power flow equations.

The Taylor series expansion of (2) turns out to be

ys= y(xe) + JΔx + y(Δx)------(3)

Where xe: Estimate of x

J: Jacobian matrix

Δx: Error (Correction vector)

Namely, it can be expressed up to the third term completely and the final term has the same form but different variable as the first term.

A good initial guess $x^{(0)}$ is needed to start the iterative process. Typically a flat start is an acceptable initial guess [14]. The algorithm stops if the variable increments Δx are lower than a given tolerance ε or number of iterations is

greater than a given limit ($i>i_{max}$). In the later case, the algorithm has likely failed to converge. For well conditioned cases, the standard NR technique typically converges in 4-5 iterations. However NR technique will fail to converge in case of ill-conditioned systems..

III. RK4 Method

It is well known that the forward Euler method, even with the variable time step, can be numerically unstable. Reference [9] suggests that given analogy between the power flow equations (1) and ODE (2), any well-assessed numerical method can be used to integrate (2). It is thus intriguing to use some efficient integration method for solving (1).Observe that, since the computation of $f=-[g]^{-1}g$ implies the inversion of power flow Jacobain matrix, only explicit integration methods are suitable and computationally efficient, since one does not need to compute the Jacobian matrix of f.

$$\dot{x} = f(x) \text{ ----(4)}$$

For the sake of example, in the sake study described in case study, we use classical fourth order Runge-Kutta formula(RK4). A generic step of the RK4 is as follows:

$$k_1=f(x^{(i)}) \text{ ------(5)}$$
$$k_2=f(x^{(i)}+0.5\Delta t k_1)$$
$$k_3=f(x^{(i)}+0.5\Delta t k_2)$$
$$k_4=f(x^{(i)}+0.5\Delta t k_3)$$
$$x^{(i+1)}=x^{(i)}+\Delta t(k_1+ 2k_2+ 2k_3+ k_4)/6$$

The time step Δt can be adopted based on the estimated truncation error of integration method. An interesting discussion on Runge-Kutta truncation error estimation can be found in [10]. For example, RK4 error can be estimated based on half step method, as follows:

$$\xi = \max(\text{abs}(k_2-x^{(i+1)})) \text{ ----------(6)}$$

Then the time step Δt can be computed based on the following simple heuristic rules.

If $\xi > 0.01$ then $\Delta t=\max(0.985\Delta t,0.75)$ --(7)

If $\xi \leq 0.01$ then $\Delta t=\min(1.015\Delta t,0.75)$

Based on these rules, the time step is increased if the truncation is greater than a given threshold and decreased if the truncation error is lower than a given threshold. The minimum value of time step is limited to 0.75. If the lower value of time step Δt is not limited, in case of unsolvable power flow problems, the proposed algorithm provides a solution close to the feasibility boundary of power flow equations, as discussed in [11]. All thresholds and tuning parameters in (7) have been determined based on heuristic criteria.

It is important to note that any order and any version of the family of Runge-Kutta formulas could be used, and any of these methods is numerically more stable than the Euler forward method.

Steps to implement RK

1. Initialize $x^{(0)}$ and set iteration count i=1,Δt=1
2. solve (4)
3. if ε is greater than max(abs($\Delta x^{(i)}$)) , then stop the iterations. Otherwise go to step 4
4. Update Δt using (6) and increment iteration count by 1.
5. If iteration count is more than maximum no.of iterations then stop the iterations. Otherwise go to step (2)

IV IWAMOTO METHOD

Load Flow Problem by Nonlinear Programming Formulation

The load flow problem using the nonlinear programming formulation was suggested by Wallach and Sasson, and since then many investigations were made. The main points are as follows.

(1) Determine the form of the cost function F(r) in a least squared sense.
(2) Determine the estimate value xe (r)
(3) Determine the direction of the correction vector Δx(r) so that the value of the cost function decreases
(4) Determine the scalar multiplier μ(r) so that the cost function decreases, and multiply it by the correction vector Δx(r).
(5) Calculate the new estimate value xe (r+l) = xe(r) + μ(r) Δx(r)
(6) If the solution converged stop the computation, and if not set r=r+l and go to the step (2).
Attention is paid particularly in the formulation of step (4) .In order to find the scalar multiplier p μ(r), many studies have been carried out.
However, no decisive method has been so far found. Because the scalar multiplier μ(r) has no special name, we call the optimal value among the μ's "the optimal multiplier" in this paper.

Derivation of the Proposed Optimal Multiplier

The number of the iteration counts is restricted to r. Therefore, the subscript (r) expressing the iteration number is omitted.

Suppose that the correction vector Δx is obtained by some way, let us derive the optimal multiplier. Moving all the right-hand side of (3) to the 1eft hand side, we have

ys-y(xe)-JΔx-y(Δx)=0 ----------(8)

In order to adjust the length of the correction vector Δx, we multiply the scalar quantity μ by Δx. Then it follows that.

ys-y(xe)-JμΔx-y(μΔx)=0----------(9)

In the above equation, μ in the third term can appear in front of J being a scalar, and the forth term can become $\mu^2 y(\Delta x)$ using (2), that is

ys-y(xe)-μJΔx-μ^2y(Δx)=0----------(10)

Here we define the vectors a,b,c for simplicity, as follows.

$$a = \begin{bmatrix} a_1 \\ . \\ . \\ . \\ a_n \end{bmatrix} = y_s - y(x_e), b = \begin{bmatrix} b_1 \\ . \\ . \\ . \\ b_n \end{bmatrix} = -J\Delta x, c = \begin{bmatrix} c_1 \\ . \\ . \\ . \\ c_n \end{bmatrix} = -y(\Delta x)$$

------(11)

Then, eq(10) can be written simply as below

a+μb+μ^2c=0 ------(12)

In order to determine the value of the μ in a least squared sense, the following cost function is considered.

$$\text{Minimize } F = \frac{1}{2}\sum_{i=1}^{n}\left(a_i + \mu b_i + \mu^2 c_i\right)^2 \text{ -(13)}$$

The optimal solution μ* of the above equation can obtained by solving the equation below.

$$\frac{\partial F}{\partial \mu} = 0 \text{ ---------(14)}$$

Namely,

$$g_0 + g_1\mu + g_2\mu^2 + g_3\mu^3 = 0 \text{ --------(15)}$$

where

$$g_0 = \sum_{i=1}^{n}\left(a_i b_i\right), g_1 = \sum_{i=1}^{n}\left(b_i^2 + 2a_i c_i\right)$$

$$g_2 = 3\sum_{i=1}^{n}\left(b_i c_i\right), g_3 = 2\sum_{i=1}^{n} c_i^2 \quad \text{-------(16)}$$

It can be easily observed that the equation (15) is a scalar cubic equation with respect to μ. Thus the equation can be solved easily by Cardan's formula analytically.

Application of The Optimal Multiplier to The N-R Method

The most widely used AC load flow calculation method is the N-R method, and our examination showed also that the application of the optimal multiplier to the N-R method was most effective[18].Thus, we describe here how to apply the optimal multiplier to the N-R method. If applied to the N-R method, the solution never diverges but converges in such a manner that the value of the cost function always decreases [19].

In the N-R method, the correction vector Δx(r) is obtained basically by triangulating the matrix J(r) in the following equation.

ys-y(xe(r))=J(r)Δx(r) ------(17)

The quantities required for calculating the optimal multiplier μ(r) * are given by (7) as below.

a(r)=ys-y(xe(r)) -------(18)

b(r)=-J(r)Δx(r)=-a(r) -------(19)

c(r)=-y(Δx(r)) -------(20)

Note the important fact that b(r)=-a(r) in (19). These calculations are carried out automatically in the process of the N-R method, and thus no additional calculations are necessarily required for them.

Flowchart

The flowchart of the proposed method is shown in Fig. 2.

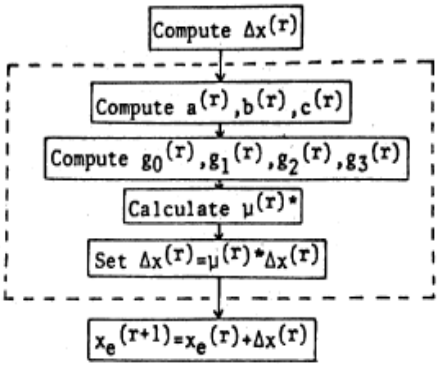

Fig 2 Flowchart

The readers who have the N-R program (in rectangular coordinates) can only make a subroutine for the dotted portion and add it to their programs. Namely, after calculating the correction vector Δx(r), do not add it to the

current estimate x (r) to get the new estimate xe (r+l) but add μ(r) *Δx(r) to xe (r).

V.MODELING OF FACTS DEVICES

General

The Runge–kutta method and IWAMOTO optimal multiplier methods developed in previous section are extended to include FACTS devices (SVC,TCSC,STATCOM,UPFC) together with their steady state modeling without difficulty.

SVC

The SVC is taken to be a continuous, variable-shunt susceptance, which is adjusted in order to achieve a specified voltage magnitude while satisfying constraint conditions [6].

Two models are presented in this paper:

1) SVC total susceptance model: A changing susceptance *R,,,* represents the fundamental frequency equivalent susceptance of all shunt modules making up the SVC. This model is an improved version of SVC models currently available in open literature.

2) SVC firing angle model: The equivalent susceptance *Beq***,** which is function of a changing firing angle (α), is made up of the parallel combination of a thyristor controlled reactor (TCR) equivalent admittance and a fixed capacitive susceptance. This is a new and more advanced SVC representation than those that are currently available in open literature. This model provides information on the SVC firing angle required to achieve a given level of compensation.

VI. SVC LOAD FLOW MODELS

In practice the SVC can be seen as an adjustable reactance with either firing angle limits or reactance limits. The circuit shown in Fig. 1 is used to derive the SVC's nonlinear power equations and the linearized equations required by Newton's method [4].

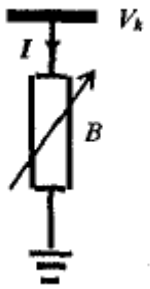

Fig. 1. Variable shunt susceptance

In general, the transfer admittance equation for the variable shunt compensator is,

$I = jBV_k$ ----------(21)

and the reactive power equation is,

$Q, = -V_k^2 B$

Linearized, positive sequence SVC models for Newton-Raphson load flows are presented in this section.

A.SVC Total Susceptance Model (B = B_{SVC})

The linearized equation of the SVC is given by (22), where the total susceptance B_{SVC} is taken to be the state variable,

$$\begin{bmatrix} \Delta P_k \\ \Delta Q_k \end{bmatrix}^i = \begin{bmatrix} 0 & 0 \\ 0 & Q_k \end{bmatrix}^i \begin{bmatrix} \Delta \theta_k \\ \Delta B_{svc} / B_{svc} \end{bmatrix} \text{-(22)}$$

At the end *of* iteration i**,** the variable shunt susceptance BSVC is updated according to (23),

$$B_{svc}^{i+1} = B_{svc}^i + \left(\Delta B_{svc} / B_{svc}\right)^i B_{svc}^i \text{ -----(23)}$$

This changing susceptance represents the total SVC susceptance necessary to maintain the nodal voltage magnitude at the specified value. Once the level of compensation has been determined, the firing angle required to achieve such compensation level can be calculated. This assumes that the SVC is represented by the structure shown in Fig. 2. Since the SVC susceptance given by (23) is a transcendental equation, the computation of the firing angle value is determined by iteration.

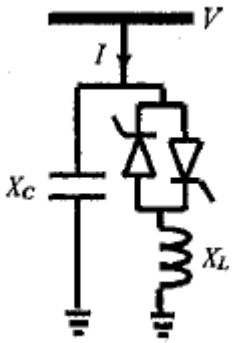

Fig.2. SVC structure

B. SVC Firing Angle Model (B=B_{eq})

Provided the SVC can be represented by the structure shown in Fig.2, it is possible to consider the firing angle to be the state variable. In this case, the linearized SVC equation is given as,

$$\begin{bmatrix}\Delta P_k\\ \Delta Q_k\end{bmatrix}^i=\begin{bmatrix}0 & 0\\ 0 & Q_k\end{bmatrix}^i\begin{bmatrix}\Delta\theta_k\\ \alpha\end{bmatrix}^i \text{------(24)}$$

where

$$\frac{\partial Q_k}{\partial\alpha}=\frac{2V_k^2}{X_L}\left(\cos(2\alpha)-1\right)\text{-------(25)}$$

At the end of iteration *i,* the variable firing angle α is updated according to (26),

$$\alpha^{i+1}=\alpha^i+\Delta\alpha^i \text{----------(26)}$$

and the new SVC susceptance B_{eq} is calculated from (24).

It should be remarked that both models, the total susceptance model and the firing angle model observe good numerical properties. However, the former model requires of an additional iterative procedure, after the load flow solution has converged, to determine the firing angle. Hence, their mathematical formulations are quite different. Accurate information about the SVC firing angle, as given by the load flow solution, is of paramount important in harmonics and electromagnetic transients studies [5].

VII. Thyristor Controlled Series Compensators (TCSC)

Thyristor-controlled series compensators (TCSC) are connected in series with the lines. The effect of a TCSC on the network can be seen as a controllable reactance inserted in the related transmission line that compensates for the inductive reactance of the line. This reduces the transfer reactance between the buses to which the line is connected. This leads to an increase in the maximum power that can be transferred on that line in addition to a reduction in the effective reactive power losses. The series capacitors also contribute to an improvement in the voltage profiles.

A.TCSC Power Flow Model

The admittance matrix of the TCSC module shown in Fig.3 is,

$$\begin{bmatrix}I_k\\ I_m\end{bmatrix}=\begin{bmatrix}jB_{kk} & jB_{km}\\ jB_{km} & jB_{mm}\end{bmatrix}\begin{bmatrix}V_k\\ V_m\end{bmatrix}\text{--------(27)}$$

where

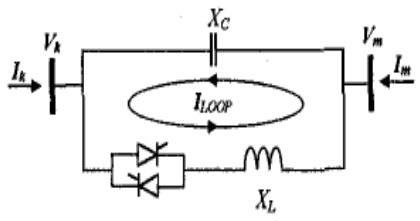

Fig. 3. TCSC module

$$B_{km}=B_{mk}=B_{TCSC(1)}=\frac{1}{X_{TCSC(1)}}\text{ -----(28)}$$

The TCSC power equations at node *k* are,

$$P_k=-V_kV_mB_{TCSC(1)}\sin(\left(\theta_k-\theta_m\right))\text{-----(29)}$$

$$Q_k=--V_k^2B_{TCSC(1)}+V_kV_mB_{TCSC(1)}\cos\left(\theta_k-\theta_m\right)\text{----------(30)}$$

The TCSC linearized power equations with respect to the firing angle are,

$$\frac{\partial P_k}{\partial\alpha}=P_kB_{TCSC(1)}\frac{\partial X_{TCSC(1)}}{\partial\alpha}\text{ ---------(31)}$$

$$\frac{\partial Q_k}{\partial\alpha}=Q_kB_{TCSC(1)}\frac{\partial X_{TCSC(1)}}{\partial\alpha}\text{--------(32)}$$

where

$$\frac{\partial B_{TCSC(1)}}{\partial\alpha}=B_{TCSC(1)}^2\frac{\partial X_{TCSC(1)}}{\partial\alpha}\text{-------(33)}$$

$$\frac{\partial X_{TCSC(1)}}{\partial\alpha}=-2C_1(1+\cos(2\alpha))+C_2\sin(2\alpha)(\varpi\tan(\varpi(\pi-\alpha))-\tan\alpha)$$
$$+C_2\left(\varpi^2\frac{\cos^2(\pi-\alpha)}{\cos^2(\varpi(\pi-\alpha))}-1\right)\text{------(34)}$$

For the equations at node m exchange the subscripts k and m in (29)-(32).

When the TCSC module is controlling the active power flowing from nodes k to m, at a specified value, the set of linearized power flow equations is,

$$\begin{bmatrix}\Delta P_k\\ \Delta P_m\\ \Delta Q_k\\ \Delta Q_m\\ \Delta P_{km}\end{bmatrix}^i=\begin{bmatrix}\frac{\partial P_k}{\partial\theta_k} & \frac{\partial P_k}{\partial\theta_m} & \frac{\partial P_k}{\partial V_k}V_k & \frac{\partial P_k}{\partial V_m}V_m & \frac{\partial P_k}{\partial\alpha}\\ \frac{\partial P_m}{\partial\theta_k} & \frac{\partial P_m}{\partial\theta_m} & \frac{\partial P_m}{\partial V_k}V_k & \frac{\partial P_m}{\partial V_m}V_m & \frac{\partial P_m}{\partial\alpha}\\ \frac{\partial Q_k}{\partial\theta_k} & \frac{\partial Q_k}{\partial\theta_m} & \frac{\partial Q_k}{\partial V_k}V_k & \frac{\partial Q_k}{\partial V_m}V_m & \frac{\partial Q_k}{\partial\alpha}\\ \frac{\partial Q_m}{\partial\theta_k} & \frac{\partial Q_m}{\partial\theta_m} & \frac{\partial Q_m}{\partial V_k}V_k & \frac{\partial Q_m}{\partial V_m}V_m & \frac{\partial Q_m}{\partial\alpha}\\ \frac{\partial P_{km}^{\alpha}}{\partial\theta_k} & \frac{\partial P_{km}^{\alpha}}{\partial\theta_m} & \frac{\partial P_{km}^{\alpha}}{\partial V_k}V_k & \frac{\partial P_{km}^{\alpha}}{\partial V_m}V_m & \frac{\partial P_{km}^{\alpha}}{\partial\alpha}\end{bmatrix}\begin{bmatrix}\Delta\theta_k\\ \Delta\theta_m\\ \frac{\Delta V_k}{V_k}\\ \frac{\Delta V_m}{V_m}\\ \Delta\alpha\end{bmatrix}$$

---------- (35)

where superscript *i* indicates iteration, $\Delta P_{km}=P_{km}^{\alpha,reg}-P_{km}^{\alpha}$ is the active power flow mismatch for the TCSC module, $\Delta\alpha=\alpha^{i+1}-\alpha^i$, is the incremental change in the TCSC's firing angle and $P_{km}^{\alpha}=P_k$

B. TCSC Impedance as a Function of the Firing Angle

As expected, the behavior of the TCSC power flow model is influenced greatly by the number of resonant points in the TCSC impedance-firing angle characteristic, in the range of 90-180°. Equation (35) may be used to determine the number of resonant points (poles) in a TCSC [2]:

$$\alpha = \pi\left(1 - \frac{(2n-1)\varpi\sqrt{LC}}{2}\right) \text{ where n=1,2,3,……}$$

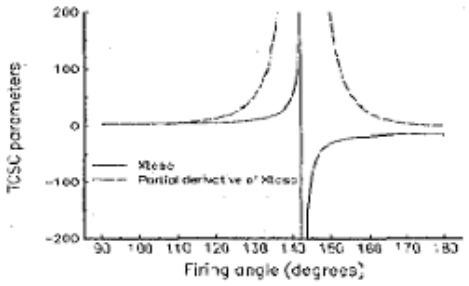

Fig. 4. $X_{TCSC(1)}$ and $\frac{\partial X_{TCSC(1)}}{\partial \alpha}$ profiles as a function of firing angle

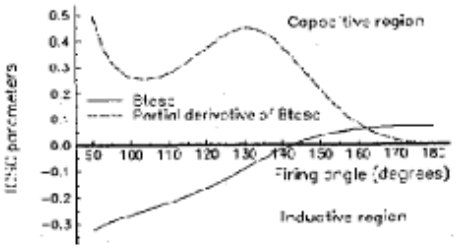

Fig 5. $B_{TCSC(1)}$ and $\frac{\partial B_{TCSC(1)}}{\partial \alpha}$ profiles as a function of firing angle

Figs. 4 and 5 show the fundamental frequency TCSC reactance and susceptance profiles, as function of the firing angle, respectively. The partial derivatives of these parameters with respect to the firing angle are also shown in these figures.

As shown in Fig. 3**,** a resonant point exists at α_R= 142.81^0. This pole defines the transition from the inductive to the capacitive regions.

It should be noted that near the resonant point, small variations of the firing angle will induce large changes in

both $X_{TCSC(1)}$ and $\frac{\partial X_{TCSC(1)}}{\partial \alpha}$. This, in turn, may lead to ill conditioned TCSC power equations and Jacobian terms[3]. On the other hand, it can he observed from Fig. 4 that the $B_{TCSC(1)}$ and $\frac{\partial B_{TCSC(1)}}{\partial \alpha}$ profiles do not present discontinuities. Both curves vary in a continuous, smooth fashion in both operative regions.

VII. UNIFIED POWER FLOW CONTROLLER (UPFC)

The UPFC is the most versatile FACTS controller with capabilities of voltage Regulation, series compensation, and phase shifting. The UPFC is able to control simultaneously or selectively all the parameters affecting power flow patterns in a transmission network, including voltage magnitudes and phases, and real and reactive powers. These basic capabilities make the UPFC the most powerful device in the present day transmission and control systems. As shown in Fig.6, the UPFC consists of two voltage-sourced converters, one in series and one in shunt, both using Gate Turn-Off (GTO) thyristor valves and operated from a common dc storage capacitor.

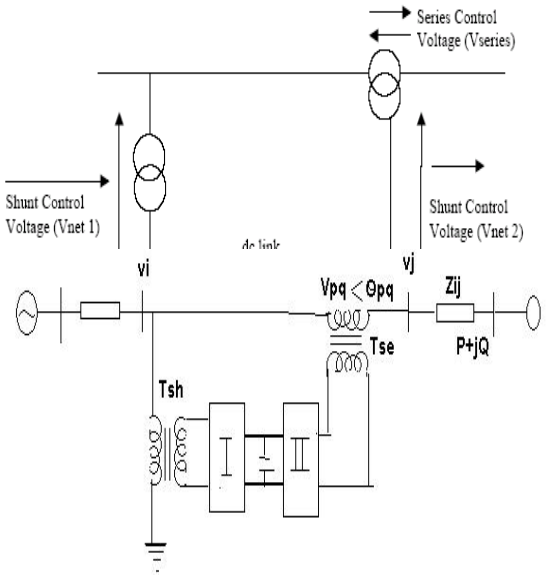

Fig.7 Representation of UPFC.

Steady state UPFC representation:

The UPFC can be represented in steady state by the two voltage sources with appropriate impedance as shown in fig.8, the voltage source can be represented by the relation ship between the voltage and amplitude modulation ratios and phase shift of UPFC. In this model the shunt transformer impedance and the transmission line impedance including the series transformer are assumed to be constant.

No power loss is considered within the UPFC. However, the proposed model and algorithm can easily include these when required.

C. Power injection model of UPFC:

The two voltage source model of the UPFC is converted into power injection the advantages of power injection is that it does not destroy the symmetric characteristics of the admittance matrix.

STEP1**:** to transform the shunt side of UPFC into a power injection at bus bar I only

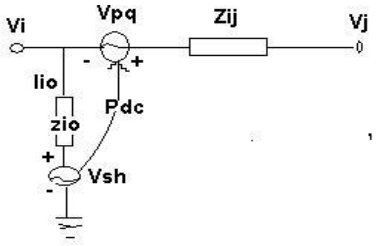

Fig.8 Steady state UPFC

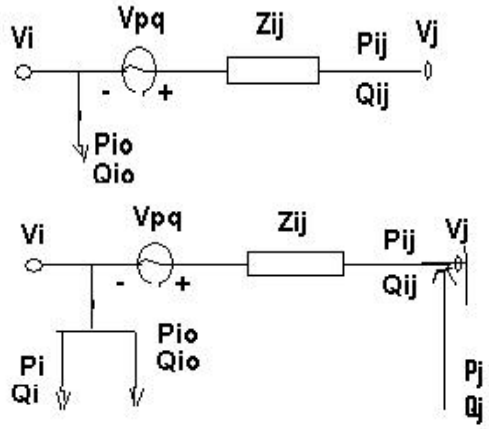

Fig. 10 Series side of UPFC into power injection model

$$P_{io} = G_{io} * V_i^2 - V_i * V_{sh} * G_{io} * Cos(\phi_{sh} - \delta_i) + V_i * V_{sh} * B_{io} * Sin(\phi_{sh} - \delta_i) - - - (36)$$

$$Q_{io} = -B_{io} * V_i^2 - V_i * V_{sh} * G_{io} * Sin(\phi_{sh} - \delta_i) + V_i * V_{sh} * B_{io} * Cos(\phi_{sh} - \delta_i) - - - (37)$$

STEP 2: second step is to convert the series source of UPFC into power injection at both bus bar I and j, which is shown in fig 10. There fore, we have

Si = Pi+jQi

$$P_i = V_i * V_{pq} * B_{ij} Sin(\theta_{pq} - \delta_i) - V_i * V_{pq} * G_{ij} Cos(\theta_{pq} - \delta_i) - - - (38)$$

$$Q_i = V_i * V_{pq} * B_{ij} Cos(\theta_{pq} - \delta_i) + V_i * V_{pq} * G_{ij} Sin(\theta_{pq} - \delta_i) - - - (39)$$

Sj=Pj+jQ

$$P_j = V_j * V_{pq} * G_{ij} Cos(\theta_{pq} - \delta_j) - V_j * V_{pq} * B_{ij} Sin(\theta_{pq} - \delta_j) - - - (40)$$

$$Q_j = -V_j * V_{pq} * G_{ij} Sin(\theta_{pq} - \delta_j) - V_j * V_{pq} * B_{ij} Cos(\theta_{pq} - \delta_j) - - - (41)$$

But the power transfer from shunt side to series side, is Pdc,

$$P_{dc} = \left(G_{ij} - jB_{ij}\right) \begin{bmatrix} V_{pq} \angle \theta_{pq} V_i \angle -\delta_i + V_{pq}^2 \\ -V_{pq} \angle \theta_{pq} V_j \angle -\delta_j \end{bmatrix}$$

When the power loss inside the UPFC is neglected then Pdc=Pio then,

Pi=Pi-Pio ;Qi=Qi-Qio

Thus the two power injections (Pi,Qi) and (Pj,Qj) represents all features of the steady state UPFC model[17]

VIII. STATIC SYNCHRONOUS COMPENSATOR (STATCOM)

STATCOM is a same type of shunt compensator FACTS device. The principle of STATCOM is the reactive power compensation which the reactive power and voltage magnitude of system can be adjusted [15]. It consists of three paths: transformer, voltage source converter (VSC), and capacitor. The reactive power is distributed in power system by the converter control.

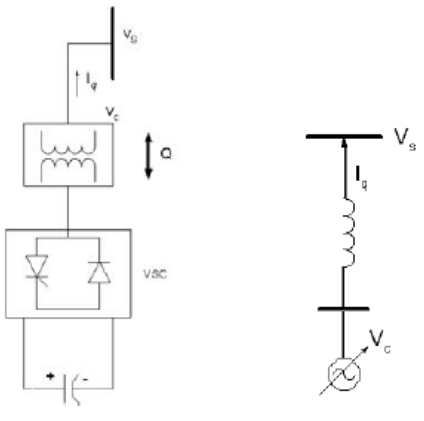

Fig 11a: The STATCOM

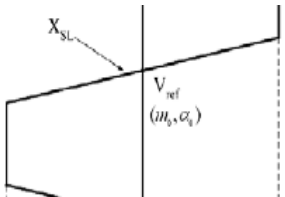

From Fig. 11, the characteristic of STATCOM shows the status of STATCOM either inductive or capacitive which is depended on the converter voltage adjustment [16].

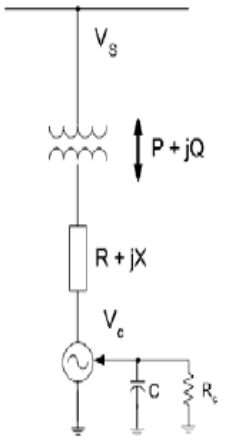

Fig 12: The equivalent circuit of STATCOM.

The ed as:

$$V_{dc} \quad CV_{dc} \quad R_c C \quad CV^2 V_{dc}^{2}) \quad \text{--- (42)}$$

The power injection at A.C. bus has the following form**:**

$$P = V^2 G - kV_{dc} VG\cos(\theta-\alpha) - kV_{dc} B\sin(\theta-\alpha)$$

---- (43)

$$Q = -V^2 B - kV_{dc} VB\cos(\theta-\alpha) - kV_{dc} G\sin(\theta-\alpha)$$

---- (44)

where

G: the conductance of STATCOM and

B: the susceptance of STATCOM.

IX. Case Study

A 13 bus ill conditioned test system incorporating the mathematical models of FACTS devices. An in depth description of the test system is given in [12].

SVC Specifications: A shunt connected SVC models are incorporated for the test system where SVC is connected to the bus-9 with the following specifications

Susceptance model: Susceptance (B_{svc}) =0.02 pu; Its Lower and Upper limits are [-0.25; 0.25].

***Firing angle model*:** In case of firing angle model the specifications are: Capacitive reactance=1.07; Inductive reactance=0.288; Initial firing angle=140^0 with lower and upper limits [90; 180]. In both models the bus voltage is set to hold at 1 pu.

TCSC Specifications: A series connected FACTS device TCSC is connected between buses 10 and 11 since R/X ratio of line connecting these buses is very low. Both power flow model and firing angle model are used with following specifications.

TCSC Power Flow model:

Susceptance=-0.05 and its lower &upper limits=[-.09 .09]; Power required to flow in the line=0.10 pu;

TCSC firing angle Model:

Capacitive reactance= 0.009375; Inductive reactance=0.01625. Initial firing angle=140^0 and its lower &upper limits=[90 180]; Power required to flow in the line=0.10 pu;

UPFC Specifications: UPFC is connected between lines 3 and 4 with shunt source voltage of 1 per unit and shunt source reactance 0.015 and specified power flow in the series converter is set to 0.21 per unit and series reactance set to 0.05.

STATCOM Specifications: Statcom is connected to bus 7 with a target voltage value of 1 per unit and with it's upper and lower voltage limits set to 1.1 and 0.95 All these models are implemented using proposed method for obtaining the load flow solution.

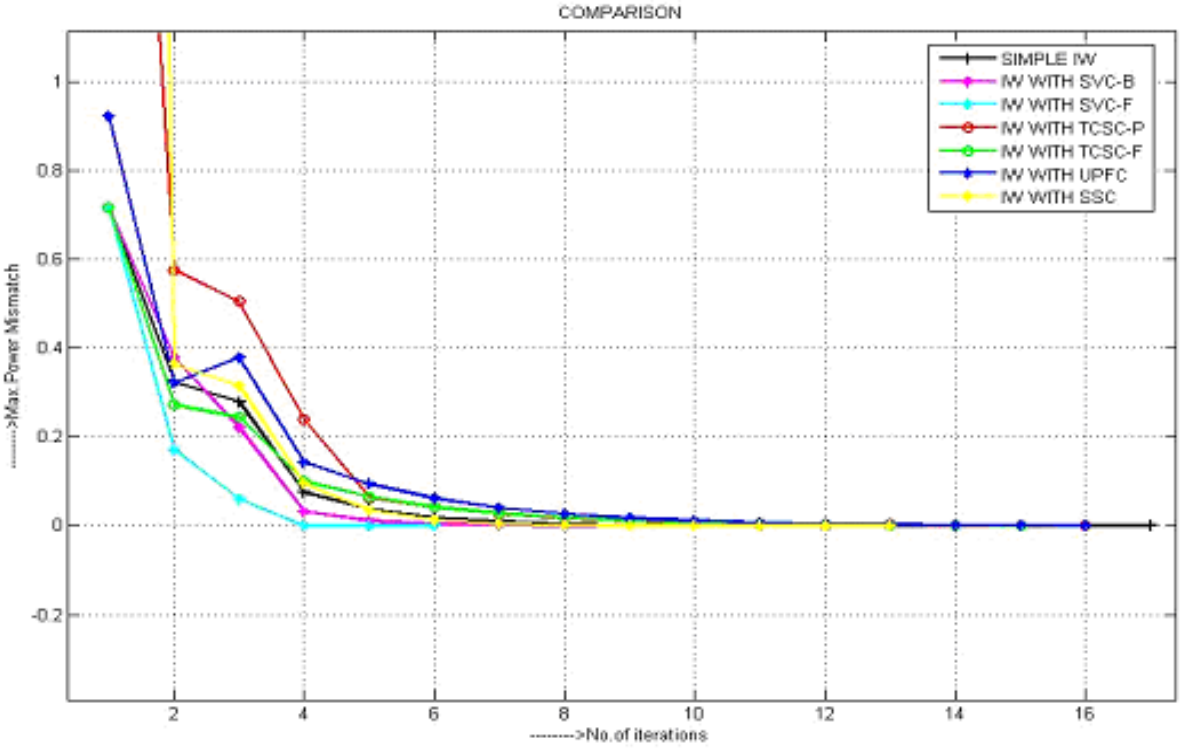

Fig 13 comparision of maximum power mismatches using IWAMOTO's method

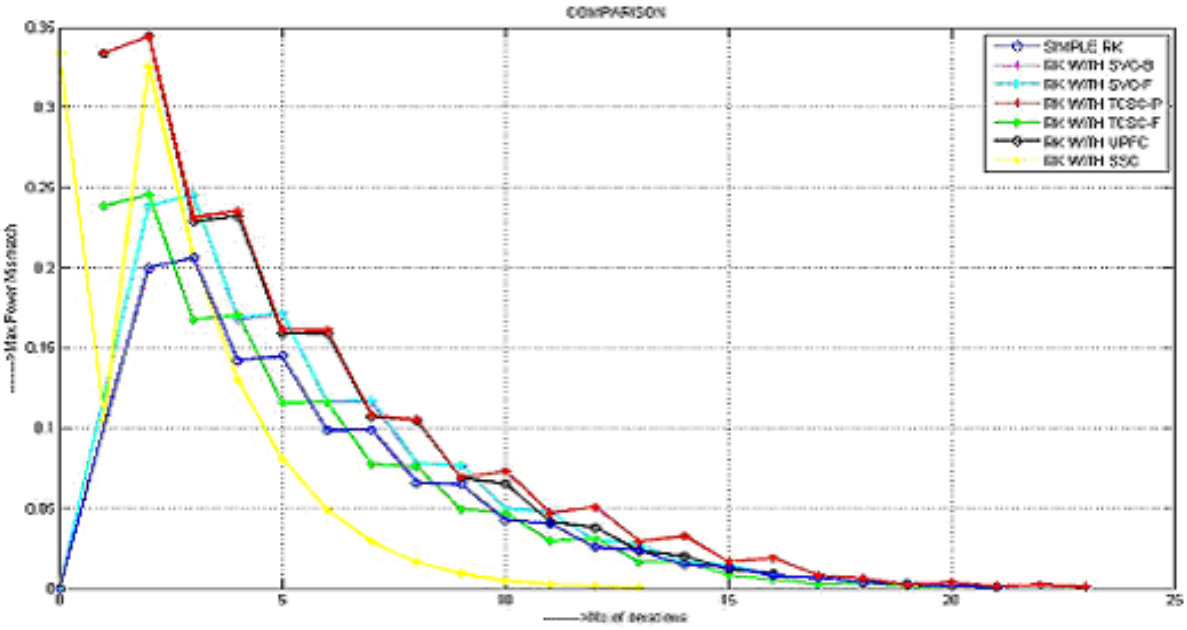

Fig 14.comparision of maximum power mismatches using Runge-Kutta method

X. RESULTS AND DISCUSSIONS

A 13-bus ill conditioned system was considered as a test system and power flow solution does not converge using Newton Raphson method. Solution was obtained by the proposed RK4 method and IWAMOTO optimal multiplier method with and without devices. The facts devices SVC TCSC, STATCOM, UPFC along with their steady state mathematical models converged using the above methods and their functional capabilities are tested by choosing suitable initial values. Selection of initial conditions makes the solution to converge, so proper selection of suitable initial values is essential. The heaviest computational part of any power flow solution technique is the factorization of the Jacobian matrix of the system. In case of IWAMOTO's method, the Jacobian matrix is factorized once per iteration while in the case of RK-4 method 4 times per iteration. Figure (13) and (14) shows the comparison of the convergence error for the iwamoto's method and proposed RK-4 method. The proposed RK-4 method always gives smaller convergence errors .The computational time required to obtain the solution is also less for the proposed RK-4 method.

CONCLUSIONS

This paper proposes efficient numerical techniques for solving ill condition power system by using RK4 and iwamoto's methods. From the results we can conclude RK4 method is best suited for solving ill conditioned power systems with and without facts devices. Future work will concentrate on using homotopy method for solving ill conditioned power systems with FACTS devices.

REFERENCES

[1] J.B. Ward and H.W. Hale, "Digital computer solution of power flow problems", AIEE Trans, (Power App. Syst.), vol. 75, pp. 398-404, June 1956.

[2] N. Christl, R. Hedin, K. Sadek, P. Lutzelberger, P.E. Krause, S. M. McKenna, A. H. Montoya, and D. Togerson, "Advanced series compensation (ASC) with thyristor controlled impedance", in Int. Conf. Large High Voltage Electric Systems (CIGRE), Paris, Sept. 1992, Paper 14/37/38-05.

[3]. C. R. Fuerte-Esquivel, E. Acha, and H. Ambriz-Perez, "A Thyristor Controlled Series Compensator Model for the Power Flow Solution of Practical Power Networks", IEEE transactions on power systems. Vol. Is, no. 1, february 2000

[4] C. R. Fuerte-Esquivel and E. Acha, "A Newton-type algorithm for the control of power flow in electrical power networks", IEEE Trans. Power Systems, vol. 12,no. 4,pp. 1474-1480,Nov. 1997.

[5] J. J. Rico, E. Acha, and T.J.H. Miller, "Harmonic domain modeling of three phase thyristor-controlled reactors by means of switching vectors and discrete convolutions", IEEE trans. on Power Delivery, vol. I I, no. 3, pp. 1678-1684, July 1996.

[6] H. Amhriz-Perez, E. Acha, and C. R. Fuerte-Esquivel "Advanced SVC Models for Newton-Raphson Load Flow and Newton Optimal Power Flow Studies", IEEE transactions on power systems. Vol. 15. No. 1, february 2000

[7] J.E. Van Ness, "Iteration method for digital load flow studies", AIEE Trans. (Power App. Syst.), vol.78, pp. 583-588, Aug 1959.

[8] W.F. Tinney and C.E. Hart, "Power flow solution by Newton's method", IEEE Trans. Power App. Syst., vol. PAS-86, pp. 1449-1456, Nov. 1967.

[9] S. M. Hetzler, "A Continuous Version of Newton's Method", *The College Mathematical Journal*, vol. 28, no. 5, pp. 348–351, Nov. 1997.

[10] L. F. Shampine, "Some Practical Runge-Kutta Formulas," *Mathematics of Computation*, vol. 46, no. 173, pp. 135–150, 1986.

[11] T. J. Overbye, "A Power Flow Measure for Unsolvable Cases" *IEEE Transactions on Power Systems*, vol. 9, no. 3, pp. 1359–1365, Aug 1994.

[12] S.C. Tripathy, G. Durga Prasad, O.P. Malik G.S. Hope, "load-flow solutions for ill-conditioned power systems by a Newton-like method", IEEE Transactions on Power Apparatus and Systems, Vol. PAS-101, No. 10 October 1982.

[13] W. F. Tinney and C. E. Hart, "Power Flow Solution by Newton's Method," *IEEE Transactions on Power Apparatus and Systems*, vol. PAS-86, pp. 1449–1460, Nov. 1967.

[14] B. Stott, "Effective Starting Process for Newton-Raphson Load Flows," *Proc. Inst. Elect. Eng.*, vol. 118, no. 8, pp. 983–987, Aug 1971.

[15] U.Eminoglu, S.A. Asun, TAlcinoz, "Application of SVC on dynamic load for different load types", proceeding of UPEC 2004, Bristol, UK (2004).

[16] N.G.Hingorani, "Understanding FACTS: concepts and technology of Flexible AC Transmission Systems", IEEE press (2000).
[17] Young Hua Song & Allan T Johns, "Flexible AC Transmission Systems (FACTS)", the institution of electrical engineering, London, United Kingdom (1999).
[18] S. Iwamoto and Y. Tamura, "A fast load flow method retaining nonlinearity," IEEE Trans. Power App. Syst., vol. PAS-97, pp. 1586-1599, Sep/Oct 1978
[19] A.M. Sasson, C. Trevino, and F. Aboytes, "Improved Newton' s load flow through a minimization technique," IEEE Trans. Power App. Syst., vol. PAS-90, pp. 1974- 1981, Sep-/Oct 1971.

.

S.Suresh Reddy received B.tech from Institution of Engineers India, received M.tech from JNTU Hyderabad and currently working as Associate Professor in NBKRIST, India.
Email:sanna_suresh@rediffmail.com
Phone:+91-9440520130

S.Sarat Kumar received B.tech from V.R.Siddartha college of Engineering, India and received M.tech from JNTU Hyderabad, currently working as Associate professor M.V.J.R College of engineering,India.
Email:sahu_sri@yahoo.com
Phone:+91-9490252044

Dr.S.V.J.Kumar obtained B.tech and M.tech from Andhra university India, received Phd. From IIT Kanpur ,India and currently working as Professor in JNTU Hyderabad.
Email:svjkumar101@rediffmail.com
Phone:+91-9848770581